PCCP

Origin of the complex main and satellite features in Fe 2p XPS of Fe_2O_3

Journal:	*Physical Chemistry Chemical Physics*
Manuscript ID	CP-ART-10-2021-004886.R1
Article Type:	Paper
Date Submitted by the Author:	17-Jan-2022
Complete List of Authors:	Bagus, Paul; University of North Texas, Nelin, Connie; none Brundle, Christopher; C. R. Brundle and Associates Crist, B. Vincent; XPS International LLC Lahiri, Nabajit; Pacific Northwest National Laboratory Rosso, Kevin; Pacific Northwest National Laboratory, Physical Sciences Division

Origin of the complex main and satellite features in Fe 2p XPS of Fe_2O_3[†]

Paul S. Bagus[a], Connie J. Nelin[b], C. R. Brundle[c], B. Vincent Crist[d], N. Lahiri[e], and Kevin M. Rosso[e]

[a]Department of Chemistry, University of North Texas, Denton, TX 76203-5017, USA
[b]Consultant, Austin, TX 78730, USA
[c]C. R. Brundle and Associates, Soquel, CA 95073
[d]The XPS Library, Salem, OR 97306, USA
[e]Pacific Northwest National Laboratory, Richland, WA 99352, USA
[†]Electronic Supplementary Information [ESI] available

Keywords: XPS, Main and Satellite Peaks, Shake and Angular Momentum Coupling, Many Body Wavefunctions

ABSTRACT: Although the origin and assignment of the complex XPS features of the cations in ionic compounds has been the subject of extensive theoretical work, agreement with experimental observations remains insufficient for unambiguous interpretation. This paper presents a rigorous *ab initio* treatment of the main and satellite features in the Fe 2p XPS of Fe_2O_3. This has been possible using a unique methodology for the selection of orbitals that are used to form the ionic wavefunctions. This orbital selection makes it possible to treat both the angular momentum coupling of the open shell core and valence electrons as well the shake excitations from the closed shell orbitals associated with the O ligands into the valence open shell orbitals associated with the Fe 3d shell. This allows the character of the ionic states in terms of the occupations of the open shell core and valence orbitals and of the contributions of $2p_{1/2}$ and $2p_{3/2}$ ionization to the XPS intensities to be determined. Our analysis gives strong evidence that many body effects are essential for a correct description of the ionic states and, in general the states cannot be described by a single configuration over the open shell orbitals. An important consequence is that the Fe 2p XPS intensity in most of the features arises from small contributions from the ionization to many, tens to hundreds, of often unresolved ionic states. While the usual understanding of the lower binding energy main and satellite features as being dominantly from $2p_{3/2}$ ionization is confirmed, this is not the case for the higher binding energy features where $2p_{1/2}$ and $2p_{3/2}$ ionization and shake excitations in the valence space mix strongly. Furthermore, we have been able to show that a very large fraction, 88%, of the total Fe 2p XPS intensity is contained in a relatively small binding energy range of ~ 35 eV. This is relevant if one wants to extract the stoichiometry of Fe_2O_3 from Fe2p/O1s intensity ratios. Similar considerations about the importance of many-body effects are likely to be relevant for other ionic compounds as well.

I. Introduction

The origin and assignment of the XPS features of the cations in ionic compounds has been the subject of extensive theoretical studies, often with controversial results that were not in

agreement. They are described as complex because there are more features with significant intensity than one would expect simply of the basis of ionizing the spin-orbit split core levels. The original assignments of the XPS of 3d compounds was based on the properties of isolated cations to model the compounds; see, for example, Refs. [1-4]. In this work the emphasis was placed on the angular momentum coupling of the open core and valence, 3d, shells. Following this, there was work, based on calculations with a parameterized Anderson model Hamiltonian, that introduced interactions between the metal cation and its surrounding ligands; see, for example, Refs. [5-8] and the review by de Groot and Kotani.[9] In large part, this work ascribed the "main" XPS features, which are usually understood to be the most intense and the lowest binding energy, BE, features, to what were called charge transfer, CT, configurations. In contrast, the satellites were ascribed to configurations with the same valence occupation as the initial, unionized configuration. More recent work based on *ab initio* wavefunction, WF, calculations for cluster models of the oxides reached the opposite conclusion that the main peaks did not involve configurations where it was necessary to change the valence occupation; see the reviews of Refs. [10-11] However, for the most part, this *ab initio* work did not treat the satellites. The limited treatment of the XPS satellites for a few oxides [12-13] usually did not give especially good reproduction of the satellite's energies and intensities. The limited treatment did however support the alternative view of the satellites as shake features where, in addition to ionization a valence electron is excited. [14-15] The objective of the present paper is to apply a unique theoretical approach to obtain descriptions, with comparable accuracy, of both the main and satellite peaks of the Fe 2p XPS of Fe_2O_3. This makes it possible to give, for the first time, reliable descriptions of the character and number of the ionic states that comprise these XPS features. The Fe 2p spectrum of Fe_2O_3, a canonical ionic compound of diverse occurrence and

general relevance, is of interest in its own right but it is also a testing ground for the reliability of the theoretical approach that we have used. In this connection, we note that the WF methodology that we use is suitable for the analysis of the occupations of the core-excited and ionized states and we are able to determine directly the physical character of the various ionic states. [16-17] Very recent work by Kas *et al.* [18] and combines a new theoretical approach based on Green's analysis for the shake features with scaled multiplets taken from atomic calculations to predict the Fe 2p XPS of Fe_2O_3. While this "nearly *ab initio*" treatment provides a reasonably good fit to the experimental spectra, [17] it does not give an analysis of the character and electronic composition of the main and satellite XPS peaks. There have been a large number of studies using a range of different theoretical methods to describe the electronic structure of core-ionized and core-excited states; see, for example, Refs. [18-25]. However, a comparison of these methods is outside the scope of this paper which is concerned explicitly with the main and satellite features of the XPS of Fe_2O_3. In particular, with the exception of the nearly *ab initio* work of Kas *et al.* [18] these works do not address the electronic character of the XPS shake-up satellites of metal oxides and other ionic transition metal compounds.

A combined treatment of both main and satellite peaks has been difficult because the configurations that are needed to describe the states that contribute to the different features have a different character. This can be seen from the CT analysis where the initial configuration for a transition metal compound is described as d^n and there are different possible final ionic configurations, where two of these are described as $(core)^{-1}(d^n)$ and $(core)^{-1}(d^{n+1})\underline{L}$. [9] The notation $\underline{L}$ indicates that an electron has been removed from the ligand, typically an O(2p) electron, and placed into the metal cation 3d shell leading to an occupation of d^{n+1}. This is an oversimplified description of the orbitals that actually describe the compound, especially since it

neglects their covalent character (i.e., the sharing of electrons between Fe and O); see, for example, Ref. [26]. However, it does show the difficulty in an *ab initio* methodology of using a single set of orbitals to describe these two configurations since they have different occupations of the shells. In particular, the variationally best d orbitals determined for an occupation of d^n will not give as good a description of the energies of configurations which have occupations of d^{n+1}; similarly, orbitals determined for d^{n+1} are not as good to describe d^n configurations. It is common practice in the calculations of the WFs for molecular systems to variationally determine the best orbitals for each state and each configuration. [27] However, since as we show in this paper, literally hundreds of final states contribute to the Fe 2p XPS of solid Fe_2O_3, it is not possible to literally optimize the orbitals for each of the ionic states. In our previous work, we have used the orbitals to describe the core ionic states which are variationally determined for the same valence occupations as the initial state configuration; see Refs. [10-11] and references therein. However, this configuration does not represent the shake configurations needed to describe the XPS satellites. This explains why we describe more correctly the XPS of the main peaks than that of the satellites. It is also possible to use a larger number of orbitals to describe the excitations from filled ligand orbitals into unoccupied orbitals of dominantly cation character; we describe this as expanding the active space of the orbitals used to describe the valence shells. A choice of a larger number of orbitals in the active space permits a better representation of the WFs and energies of the different states in the manifold of the XPS. [12] However, expanding the orbital sets increases the complexity of the WF calculations exponentially and it cannot be done in general. Thus, we have used the orbitals variationally determined for fractional occupations of the cation d orbitals and the ligand, O(2p), orbitals. The logic is that these orbitals would represent a compromise between the orbitals that are best for the XPS "main" and best for the XPS

"satellite" features. While these orbitals may not be as good for the main peaks as the previously optimized orbitals were, our results for Fe_2O_3, as described in this paper, show that we are able to give a balanced representation of the XPS features along a large range of BEs; i.e., for the main and satellite features. Furthermore, our success for Fe_2O_3 indicates that the orbitals determined for fractional occupations may also be useful for other ionic transition metal compounds.

The outline of our paper is as follows. In the following section, Sec. II, on "Concepts and Methodology", we describe more completely the concepts of different types of regions and screening of core-holes; in particular, we explain our usage of Koopmans and shake configurations. We also describe the clusters to model Fe_2O_3 and the methods for the calculation of relativistic WFs and for the calculation of XPS intensities. In Sec. III, we present an overview of the Fe 2p XPS and of the contributions from ionization of the Fe $2p_{1/2}$ and 2p3/2 shells. We also define the two sets of WFs that we compare and contrast. One set only includes the angular momentum coupling of the open core and valence shells while the second set includes the possibility to represent shake excitations as well as the angular momentum coupling. The magnitude of the XPS intensity not included for each of these sets, described as losses, is also compared. In the following two sections, a more detailed analysis is made where we consider separate regions of the XPS features and analyze how the XPS in these regions can be characterized. In Sec. IV, we define the different regions and describe the XPS intensity, separated into intensity due to $2p_{1/2}$ and $2p_{3/2}$, in each of the regions. In Sec. V, we divide the regions into smaller groups and examine the character of the ionic states in each of these groups. In particular, this indicates the extent to which the regions can be identified as either "main" or "satellite" peaks. Finally, in Sec. VI, the conclusions of our analysis are summarized

II. Concepts and Methodology

In order to represent the ionic crystal, Fe_2O_3, we use a cluster model where the central atom is an Fe cation surrounded by its six nearest O anion neighbors, denoted as FeO_6, and embedded in a field of point charges to represent the extended Madelung potential. This cluster has a C_3 point group symmetry as appropriate for the rhombohedral crystal symmetry of hematite. See, for example, Refs. [10-11] for descriptions of the use of cluster models for the study of core-level ionizations and excitations; see Ref. [28] for a discussion of the sensitivity to the choices of embedding point charges; and see Ref. [29] for the details of the cluster model of Fe_2O_3. The properties of the initial state, often denoted as the ground state, GS, and the final, core-level ionic states are determined from the molecular orbital wavefunctions, WFs, calculated for these states; see Refs. [10-11] and references therein. In order to properly and compactly represent the relaxation or response to the core-level ionization, it is common to use two sets of orbitals, one set is variationally determined for the GS shell occupations where the core levels are fully occupied and the second set is variationally determined for a configuration where an electron has been removed from the appropriate core level. These orbitals are then used to form determinants used in configuration interaction, CI, WFs for the initial and final states. These CI WFs include, as discussed below, important many-body effects for the N-electron WFs. [10-11]

It is useful at this point to consider the nomenclature that is used to describe types of final state WFs. Koopmans' theorem, KT, is an approximation for the ionic WFs where an electron is removed from a shell but no orbitals are allowed to change. [30-32] The KT WFs are normally computed for single configuration WFs but they can also be obtained for a fairly broad class of CI WFs. [33] The KT WF is also described as a frozen orbital WF. An important and useful value of KT WFs is that they do not include the relaxation, or screening, in response to the core-

hole; hence they can be used to explicitly identify the magnitude of the screening of the core-hole ions; for the importance of screening in FeO_x compounds, see Ref. [26]. Furthermore, it is necessary to have terminology to distinguish different types of configurations. The configurations where an electron is removed from a core-shell but the occupations of other shells, or sometimes groups of shells, are not changed are described as Koopmans' Configurations, KC. For the KC, the WFs may be variationally determined in order to include the response, screening, of the core hole. However, the KC are distinguished from configurations where as well as removal of a core electron, a valence electron is excited from one level to another level. These configurations are described as shake configurations. [15, 34] These configurations have also been described, especially for oxides, as charge transfer, CT, configurations where the orbital excitation is from a filled O(2p) shell into a partially occupied cation shell. [9, 35] However, the description as CT does not take into account, in a direct way, the covalent character of the orbitals which is a major mechanism for the screening of the core-hole and, hence, has major consequences for the XPS spectra. [26] Thus, in the present work, we will use the description of features in the XPS as having shake rather than CT character; for a comparison of the two usages see Ref. [10]. It is common to associate the KC configurations with main XPS peaks and the shake configurations with XPS satellites although this assignment has been questioned based on parameterized Anderson model calculations. [9, 35] One of our important goals in this work is to provide rigorous *ab initio* characterizations of the main and satellite features for the Fe 2p XPS of Fe_2O_3.

For the orbitals to be used for the many-body WFs, we determine 4 component solutions of the Dirac-Coulomb Hamiltonian [36] where ligand field, scalar and spin-orbit, SO, relativistic effects are taken into account. The orbitals are obtained for the GS configuration and for the KC

configuration of a 2p-hole and then CI WFs are determined with these orbitals. The active orbital space for the GS involves distributing 5 electrons in all possible ways over the 10 open shell spinors and the active space for the ionic states involves distributing 5 electrons over the 6 Fe 2p spinors as well as 5 electrons over the 10 valence shell spinors. These orbitals and WFs were used in our earlier work [29] where we did not take shake satellites into account. This choice of orbitals and configurations for the CI WFs is described as SO orbitals and SO WFs to distinguish it from the more extended WFs used in the present work that take shake features into account. Here, we also consider a larger active orbital and active configuration space so that we can properly represent the satellites. A discussion of this improved active orbital and active configuration space is postponed to the following section, Sec. IV, where we give an overview of the XPS obtained with and without including the shake features. The energies of the ionic CI WFs give the BEs for ionization of the initial GS WFs.

It is common to describe orbital character with Mulliken population analyses [37-40] or related methods of orbital analysis; see, for example, Refs.[41-42]. We shall use a more reliable alternative based on the projection of atomic orbitals, normally for the cation, on the cluster orbitals. [43] For an individual atomic orbital, φ_i(atom), projected on a cluster orbital, φ_j(cluster), the projection $N_{P,j}(i)$ is

$$N_{P,j}(i) = \left| \langle \varphi_j(\text{cluster}) \right| \varphi_i(\text{atom}) \rangle \left|^2 \right. \quad (1)$$

It is common to take sums of $N_{P,j}(i)$ over the atomic shells, sums over i, and over the orbitals in the cluster, sums over j, in order to define effective atomic occupations in the cluster. Here, we consider the projections on a cluster orbital, with index j, summed over the Fe 3d shell atomic orbitals, with index i. This summed projection is denoted as N_P(3d) where the index j for the

cluster orbital will be clear from context. The value of N_P is a direct measure of the covalent character of the cluster orbital [43] where the limits of $N_P(3d)=1$ indicates a pure Fe 3d orbital without any ligand character and $N_P(3d)=0$ indicates an orbital without any 3d character. Another measure of the covalent character of φ_j(cluster) is the size of the orbital defined as

$$r_{eff}(j) = [<\varphi_j(cluster) \mid r^2 \mid \varphi_j(cluster)> \mid ^{1/2} \quad (2)$$

with larger values of r_{eff} indicating a greater covalent character. [17] A third measure of covalent character of the dominantly Fe(3d), valence open shell orbitals is the relative orbital energy, ε(rel). If the orbital energy of the lowest, most strongly bound, orbital of this set is taken as $\varepsilon(rel)=0$; larger values of ε(rel) for other orbitals indicate a greater anti-bonding, more covalent character. [44] These three measures of covalent character [11, 17] are used in the following section, Sec. III, to identify the orbitals to be used to represent the shake configurations.

The relative XPS intensities, I_{rel}, are given by the Sudden Approximation, SA. [14-15] where the summations and normalization are described in the ESI†. Plots are made of the theoretical SA intensities, normally for comparison with XPS measurements. For these plots, the theoretical intensities are broadened by a Voigt convolution [45] of a Gaussian for experimental resolution and vibrational broadening, see Ref. [46], and a Lorentzian for core-hole lifetime. Details of the broadening and the choices of the Gaussian and Lorentzian full width at half maximum, FWHM, are given in the ESI†. For the BEs, we consider a BE(rel) rather than an absolute ionization energy since this allows us to avoid adjustment between the zero of the measured XPS BEs to the vacuum zero of energy used for the theoretical energies. In effect, this means that it is not necessary to be concerned with effects like surface work functions and the spectrometer Fermi energy. [34] We define BE(rel)=0 as the energy for the lowest ionic state

with the BE(rel) for other ionic states as the difference of their energies with the lowest ionic energy. When theory and experiment are compared, there is a rigid shift to align theory and experiment and the experimental and broadened theoretical intensities are scaled so that the maxima of each have the same value; no other adjustments are made.

The WF calculations for the orbitals and for the CI WFs have been performed for a Dirac-Coulomb Hamiltonian with the DIRAC program system [47] which has been modified to interface to programs written to calculate SA intensities, and WF properties. The SA intensities are calculated rigorously taking into account the different orbitals used for the initial and ionic WFs. [48-49] The same parameters, including basis sets and cluster geometries, as used in previous work [29] were used for these WF calculations. Details of convergence are given in the ESI†

III. Overview of The Fe 2p XPS: Wavefunctions, BEs, and Intensities

There are 252 determinants for the GS d^5 CI WFs where, for the rhombohedral C_3 symmetry of $Fe2O_3$ including SO splittings, there are three two-fold degenerate low lying multiplets with tiny splittings of less than 0.02 meV. These multiplets are essentially fully occupied except at incredibly high temperatures. The next excited multiplet has a higher energy of more than 3 eV and has no Boltzmann occupation. A graphic view of the splittings of the d^5 multiplets is shown by the Tanabe-Sugano diagrams given in Griffith. [50] For the 2p-hole multiplets, the initial calculations for the orbitals were for the Fe 2p KC ion configuration. These orbitals were used to determine CI WFs where the active orbitals are the 3d spinors plus 2p spinors for the ionic states leading to 1,152 determinants for the ionic state CI WFs. As explained

in the previous section, we describe these orbitals and the CI calculations performed with them as SO since they only take into account the ligand field and spin-orbit splittings. The key property is that the SO CI WFs do not include the shake configurations needed to describe the XPS satellites. For the ionic SO WFs, all 1,152 states may be of interest. While some of them will not carry XPS SA intensity, we show in the following that a very large number of the states will carry XPS intensity which is sufficiently large to make observable contributions.

In Table I, we examine, for these SO calculations, the properties of selected orbitals to determine which orbitals may need to be involved to describe the satellites. The properties are the relative Dirac Hartree Fock, DHF, orbital energies, ε(rel), the r_{eff}, Eq.(2), and the projected 3d character in the orbitals, $N_P(3d)$, Eq.(1). These properties are direct guides to the covalent character of the orbitals. To put the values of r_{eff} in perspective, the Fe-O distances in Fe_2O_3 are ≈2Å. Thus, an orbital centered on the O anions will have an $r_{eff} \approx 2$Å. For an isolated Fe^{3+} cation, the 3d r_{eff} =0.6 Å. The orbitals whose properties are shown are the open valence shell, dominantly Fe (3d) orbitals and the closed shell orbitals of dominantly O(2p) character which have the largest $N_P(3d)$. The orbitals are grouped together when they are nearly degenerate and are described with the symmetry designation they would have if the symmetry were O_h. The orbitals are described by their dominant character, their degeneracy or near degeneracy and their approximate O_h double group Oh symmetry. [51] For the Fe(3d) orbitals, their dominant character as t_{2g} and $e_g$is also given. For the GS configuration, the $N_P(3d)$ show that the Fe(3d) orbitals have small to modest covalent character. The $N_P(3d)$=0.96 for the spin-orbit split t_{2g} orbitals show that they are nearly pure Fe(3d). The Fe(3d) orbitals with e_g symmetry have somewhat more O(2p) character although with $N_P(3d)$=0.84, they are largely Fe(3d). The small

increases in r_{eff} over the 0.6 Å for the isolated Fe^{3+} cation also show a small amount of O(2p) character; of course, r_{eff} is larger for the e_g symmetry 3d orbital since it has a larger O(2p) character. Since the open shell orbitals are nearly pure Fe(3d), the closed shell orbitals that are dominantly O(2p) will not have much Fe(3d) character. The three dominantly O(2p) orbitals with the largest Fe(3d) character are shown in Table I and their values of N(3d) are all small. Furthermore, their r_{eff} are >2.1 Å indicating that they are centered almost entirely around the O anions. It is to be expected that the importance for the GS of configurations that involve excitations from the dominantly O(2p) to the dominantly Fe(3d) depends on the magnitude of their covalency with greater importance when the covalency is larger. We have made limited tests for other oxides [12, 52] which have confirmed this expectation. Given the small extent of covalency for the GS orbitals of Fe_2O_3, we have not proceeded with any expansion of the active orbital space, beyond the Fe(2p) and Fe(3d) orbitals, for the initial state SO CI WFs.

As noted in an earlier publication, [26] the covalent character changes significantly when a core level electron is ionized. These changes are shown in Table I where the character of the Fe(3d) orbitals and one of the closed shell O(2p) orbitals optimized for the KC Fe(2p) hole configuration, denoted SO-2p ion, are compared with those for the initial state configuration. The O(2p) orbital of the 2p-hole configuration is the one which has the largest N_P(3d). The covalency of the 3d orbitals which arise from t_{2g} symmetry still have only minor covalent character as shown by their r_{eff} and N_P(3d). The values for the t_{2g} open valence shell orbitals for the 2p-hole configuration have a modest increase in r_{eff} and a modest decrease in N_P(3d) but still are nearly pure Fe(3d) orbitals. However, the increase in the covalent character of the e_g orbitals over that for the initial configuration is dramatic. The N_P(3d) now indicates that the orbital is ≈ 50% Fe(3d) and 50% O(2p). In addition, the r_{eff} for this orbital is much larger than it was in the initial

configuration. Consistent with the greater anti-bonding character for the e_g orbital for the 2p ion, its ε(rel) is ~2 eV larger than the average t_{2g} ε(rel) while for the initial configuration, before a 2p electron is ionized, it was only 1.3 eV larger. The large covalency of the e_g Fe(3d) orbitals is consistent with their spatial orientation since they are directed toward the O anions. [10] Furthermore, there is a larger covalent bonding character in the O(2p) orbital shown for the SO-2p ion configuration as shown by the increase in N_P(3d) and the decrease in r_{eff} compared to the values for the initial configuration.

These changes all suggest that we need to expand the active orbital and active CI spaces to include at least some of the O(2p) orbitals in order to include shake configurations to more accurately describe the XPS satellites. The question is how these spaces can be expanded with a limited and controlled increase in the size of the CI calculation, since the number of determinants in the calculation of the CI WFs grows exponentially with the number of orbitals in the active space. In previous work, we have used a few of the SO orbitals in the active spaces but this lead to only a small fraction of the intensity in the XPS satellites unless we included a larger number of orbitals. [12] We believe that the reason for this limitation is that the orbitals that are variationally best for the KC ionic configuration are not the best to use for configurations where there have been shake excitations. This is because the occupations, especially, of the cation d orbitals but also the anion 2p orbitals are different between the KC and shake configurations. In order to address the imbalanced description of the KC and shake configurations, we optimized orbitals for fractional occupations in the Fe(3d) and O(2p) orbital spaces. The logic is that a suitable fractional occupation will provide orbitals of comparable quality for both the KC and the shake configurations. An intuitive choice is to have a fractional occupation which is the average of the occupations for the KC and shake configurations. Although, it is possible to vary the

fractional occupation to find the best fit between theory and experiment, this procedure would bring an empirical character to our *ab initio* calculations. In the present paper, where the focus is on the character of the satellite structure of Fe_2O_3, we will consider only a single fractional occupation where 0.5 electrons moved from the O(2p) manifold to the Fe(3d) manifold. If general rules could be found to justify a different choice of fractional occupation to give a more balanced description of the main and satellite XPS features, then such a choice would be appropriate. However, the 0.5 fractional occupation which we use leads to occupations for the Fe(2p) ions of Fe_2O_3 of $Fe(2p)^5O(2p)^{35.5}Fe(3d)^{5.5}$ where only the shells of the embedded FeO_6 cluster that are not fully occupied are shown. These orbitals are described as CI14-2p ion orbitals as a shorthand for the CI active space that these orbitals will be used for as explained below. For this occupation, the O(2p) and the e_g Fe(3d) orbitals still have substantial covalent character while the covalency of the t_{2g} Fe(3d) orbitals remains rather limited.

We now consider the CI configuration space that is used with the CI14-2p ion orbitals shown in Table I. There are 14 different orbitals for the O(2p) and Fe(3d) shells shown. The CI built from these orbitals has 9 electrons distributed in all possible ways over these 14 orbitals for a total of 2002 different distributions. This is the origin of the designation as CI14. These valence distributions are combined with the 6 ways of distributing 5 electrons over the 6 Fe(2p) orbitals leading to a total of 12,012 determinants for the CI space; these determinants define the many-body space for the WFs. The Dirac-Coulomb Hamiltonian over these determinants is diagonalized to obtain 12,012 WFs for the Fe 2p ions. Even though many of these WFs will have a zero intensity from symmetry selection rules, we shall show, especially in Sec. IV, that literally hundreds of different ionic states contribute to the observed Fe 2p XPS. Furthermore, the WFs are usually combinations of many determinants as shown by the fact that the orbital occupations

in the WFs often have values that are far from integer. In other words, the WFs cannot be represented by a single determinant and the ionization usually cannot be represented as the removal of a single electron from the initial state WF. It is these two features, which are clearly manifested by the CI WFs, that are the basis for describing the XPS process for Fe_2O_3 as a many-electron process

In Fig. 1, we plot the theoretical Fe 2p XPS for Fe_2O_3 compared to our measured XPS for the two different sets of CI WFs. The measured XPS, shown as a dotted line, has the background removed following the procedure described in Ref. [29]. The theoretical XPS is shown as a solid line and the contributions of the individual 2p ionic states with the largest intensities are shown as light curves below the solid curve. The theoretical SA intensities for the individual states are Voigt broadened as described in Sec. II and the ESI†. The plots are made for the relative BEs, BE(rel), see Sec. II, in the range $-6 \le BE(rel) < 34$ eV. While for the CI14 WFs, there are states with energies up to BE(rel)=114 eV, 99.6% of the Fe 2p XPS intensity is obtained from multiplets with BE(rel)<34 eV; see Sec. IV. There is intensity in the region below BE(rel)=0 because of the Gaussian and Lorentzian broadenings of the ionizations to states at BE(rel)≈0 eV The comparison of experiment to theory for the SO 2p ion WFs is in Fig. 1(a); this is almost identical to the theoretical results published earlier [29] but it does not include certain atomic many body effects that we had found do not substantially modify the spectra. Here, the theory only includes the many-body angular momentum coupling of the Fe(2p) and Fe(3d) shells. The comparison of experiment to theory for the CI14 2p ion WFs is in Fig. 1(b). Here the theory does include the many-body shake configurations.

The SO WFs for the 2p ions do give a reasonably good description of the two main features at $0 < BE(rel) < 4$ eV, and at $13 < BE(rel) < 17$ eV; these features have traditionally been

ascribed to $2p_{3/2}$ ionization and $2p_{1/2}$ ionization, respectively; see, for example, Refs. [53-54] Our results provide the surprising result that this assignment is not entirely correct. It is clear that the observed satellites at ~ 8 eV and ~22 eV are, to a very large extent, not present using the SO WFs. However, using the CI14 WFs for the 2p ions, the comparison of theory with experiment is significantly improved since there is now intensity for the experimental features at ~9 eV and ~24 eV. While the BE's and I_{rel} of these features are not a perfect match to the measured XPS, they do, for the first time for an *ab initio* cluster model simulation, provide a reasonable representation of these XPS features. This good agreement between our theory and experiment provides strong confidence in the accuracy of the detailed analysis we make for the character and origin of the satellite as well as the main features. The theoretical representation of the first main peak is somewhat better for the SO WFs, Fig. 1(a) than for the CI14 WFs, Fig. 1(b). This is not surprising because, as we show below, this feature is dominated by the SO configurations and the SO orbitals are variationally best to describe these configurations while the CI14 orbitals are a compromise to represent both SO and shake configurations. However, note that the intensity from ionizations to the states with the largest intensities, shown as light lines in Fig. 1 represent only a fraction of the total intensity, shown as a dark line. Indeed, in many regions, all the individual intensities are much smaller than the total intensity. This is a first indication that the intensity for these BEs arises from ionizations to a very large number of final states each of which has only a very small intensity and that a one-electron description of the ionization fails completely. A more complete analysis of the number of states that contribute to the XPS intensity is made in Sec. IV.

Within the SA, it is straight forward to separate the intensity due to ionization of these subshells since one can separately sum the intensities starting from the Frozen orbital ions for

$2p_{1/2}$ and $2p_{3/2}$. [17, 29] In Fig. 2, the contributions to the XPS intensity from $2p_{3/2}$ and $2p_{1/2}$ ionization for the CI14 WFs are separated: the $2p_{3/2}$ intensity is shown as a dashed red line; the $2p_{1/2}$ as a dashed blue line; and the total intensity, from Fig. 1(b), as a solid black line. They are for the same Voigt broadening as in Fig. 1. It can be seen that $2p_{3/2}$ ionization dominates for the main and satellite features for BE(rel)<12 eV. There is also intensity for $2p_{3/2}$ ionization for BE(rel)>12 eV including in the region of BE(rel)~16 eV which is normally assigned as a $2p_{1/2}$ ionization. Furthermore, while most of the $2p_{1/2}$ intensity is in the main and satellite peaks that are normally assigned to $2p_{1/2}$ ionization, there is a small amount of $2p_{1/2}$ intensity below E(rel)=12 eV which is normally assigned to main and satellite features for $2p_{3/2}$ ionization. A more detailed analysis of the distribution of the XPS intensity will be made in Sec. IV.

In Table II, we compare the totals of the XPS intensity recovered with the SO and CI14 WFs when the SA I_{rel} are summed over all final, ionic states and summed over the Boltzmann weighted occupations of the low-lying initial states of Fe_2O_3; see, Secs. II, III and the SI. These sums are given as $I_{rel}(2p_{1/2})$, $I_{rel}(2p_{3/2})$, and $I_{rel}(2p)= I_{rel}(2p_{1/2})+I_{rel}(2p_{3/2})$. The physical significance of these sums is that they are the areas under the curves, as plotted, for example, in Fig. 2 albeit with a suitable normalization. The total SA intensities, for the normalization used, if all possible ionic states had been included in our WFs, a complete CI calculation, is given in the row of Table II labelled “Complete”. With the complete I_{rel}, it is possible to determine the XPS intensity to states not included in the manifold of SO and CI14 WFs. For the SO WFs, this intensity is conventionally described as a loss to shake states. For the CI14 WFs, the origin of the loss represents the incompleteness of these WFs and there may also be a contribution from the different screening with fractional occupations. However, even for the CI14 WFs, we shall also describe this loss as a shake loss. These losses are given in the table as a percent loss for the SO

and CI14 WFs. For both the SO and CI14 WFs, the $I_{rel}(2p_{3/2})$ are almost exactly twice the $I_{rel}(2p_{1/2})$ and thus, the losses are essentially identical for the $2p_{1/2}$ and $2p_{3/2}$ ionization. The physical driving force for the intensity to shake satellites is the rearrangement of the valence electron orbitals in the presence of the core-hole. [14-15] The equality of the losses for $2p_{1/2}$ and $2p_{3/2}$ ionizations indicates that the potential the valence electrons see is virtually identical whether a $2p_{1/2}$ or a $2p_{3/2}$ electron is removed. The fact that the ratio of the $2p_{3/2}$ XPS intensity is twice the $2p_{1/2}$ intensity is general; see, for example, Refs. [11, 55]. The data in Figs. 1 and 2 and the further analysis in the following section, show that these intensities are distributed over many states with a range of BEs. For the SO WFS, the losses are 40% indicating that this fraction of the intensity must be in shake satellites rather than in the main peaks. This shows that main peak intensities may need to be scaled by these losses to obtain information about the composition, or stoichiometry, of the material. [56-57] However, for the CI14 ionic WFs, the losses of intensity to states that are not in this extended manifold is much smaller, only 12%. Thus, the measured XPS in this relatively narrow energy range should be at least 88% of the total XPS intensity from the Fe(2p) ionization. This could provide useful information for the estimation of stoichiometry by ratioing Fe2p/O1s intensity.

IV. Distribution of XPS Intensities and Division into Regions

We have so far examined plots of the XPS intensity and shown the difference between the SO WF plots that include the angular momentum coupling and the CI14 WF plots that include features that we have described as Shake. For both the SO and CI14 WFs, spin-orbit splitting and ligand field splittings are taken into account. We now consider a detailed analysis of the character of the ionic states and origin of the SA intensities of these states as being for $2p_{1/2}$ or $2p_{3/2}$ ionization. For this analysis and to examine the detailed character of the states, it is

useful to divide the spectra into different regions. We consider four regions for the ionic states with: (1) BE(rel) in the range 0≤BE<6.0 eV; (2) BE(rel) in the range 6.0≤BE<12.0 eV; (3) BE(rel)in the range 12.0≤BE>18.0 eV; and (4) BE(rel) in the range 18.0≤BE<26.0 eV. Region (1) is typically associated with Fe ($2p_{3/2}$) ionization to Koopmans' theorem, KC, peaks; Region (2) to Fe ($2p_{3/2}$) shake or CT satellites; Region (3) to Fe ($2p_{1/2}$) KC peaks; and Region (4) to Fe ($2p_{1/2}$) shake satellites, respectively. For the justifications presented to support these assignments see, for example, Refs. [29, 58-59]. There have been alternative assignments that the CT features in the XPS of 3d TM ionic compounds are at lower BE than the KC features; see for example Refs. [9, 35]. In the present work, we will present compelling evidence from our *ab initio* WF calculations that these assignments obtained with Anderson model Hamiltonians are incorrect assignments for Fe_2O_3. For this purpose, we contrast and compare the properties of the XPS obtained with the SO ionic WFs and the CI14 ionic WFs. Related results for the properties of the Fe 2p XPS of Fe_2O_3 obtained with the SO WFs have been presented earlier [17] but we have revised the presentation of the SO WF results to exactly parallel the presentation of the CI14 WF results that include the shake satellites. This allows a direct comparison between the case where only the KC angular momentum coupling is considered and the case where shake excitations are included.

We begin with a graphical summary of the analysis of the intensities in the different regions which is shown in the plots of the summed intensity as a function of BE(rel) in Fig. 3(a) for the SO WFs and in Fig. 3(b) for the CI14 WFs. The intensity plotted in Fig. 3 is the sum of the intensities for all BEs with energy less than E. Specifically, $I_{sum}(E)$ is plotted where

$$I_{sum}(E) = \Sigma_i I(E_i); \quad (1)$$

and the sum is for all $E_i \leq E$, and I(E) is the fractional SA intensity normalized so that the limiting value of I_{sum} for Fe 2p ionization at large E is 100. As well as the total Fe 2p ionization, black curve in the figure, the contributions from ionization only of Fe $2p_{3/2}$, red curve, and only of Fe $2p_{1/2}$, blue curve, are shown. The limiting values of the $2p_{3/2}$ and $2p_{1/2}$ at large E are 66.7% and 33.3%, respectively. For the SO WF I_{sum} in Fig. 4(a), the asymptotic values are reached at BE(rel)<25 eV. As shown in Fig. 1(a), the major contributions to the Fe 2p XPS are in two features, 0≤BE(rel)<4 eV and BE(rel)~15 eV. Fig. 3(a) shows that the XPS intensity in the first region is essentially from ionization of $2p_{3/2}$ and in the second region, the intensity is almost entirely from $2p_{1/2}$ ionization. This is very much as expected. However, the distribution of the Fe 2p XPS intensity is quite different for the CI14 WFs where shake configurations have been included in the WFs.

For the CI14 WF I_{sum} in Fig. 3(b), these limiting values are almost exactly reached at E = 30 eV and essentially fully reached by E = 40 eV.-The theoretical XPS shown in the plots of SA intensity in Figs. 1 and 2 are for BE(rel)≤34 eV; hence, they show essentially all the XPS intensity contained in our CI14 active space WFs. For E between 0 and ~ 10 eV, Fig. 3(b) shows that the $2p_{3/2}$ ionization, and the total 2p ionization, are almost identical and the curve for $2p_{1/2}$ ionization is almost, but not quite identically, zero. Clearly, the XPS for this range, which includes the main low BE peak and the satellite at ~8 to 10 eV, is strongly dominated by Fe $2p_{3/2}$ ionization. For E above ~15 eV, the $2p_{1/2}$ contributions to the XPS grow rapidly and almost plateau at ~E=20 eV which includes the second, higher BE, intense peak in the Fe 2p XPS. At E~25 eV, the blue curve rises again before it reaches its asymptotic value of 33.3% which shows that the ~ 20 eV satellite is mainly from Fe $2p_{1/2}$ ionization.

The information in Fig. 3 is quantified and extended with a decomposition of the SA intensity into contributions in the 4 different regions; see Tables III and IV for the SO and CI WFs, respectively. The SA intensities summed over the states in each region are given for $I_{rel}(2p_{1/2})$ and $I_{rel}(2p_{3/2})$, separately, as well as for their sum, $I_{rel}(2p)$. These intensities are given for three thresholds for the SA intensity of an individual state to be included in the summations for the I_{rel}; the thresholds are I>0.0001, I>0.001, and I>0.005 where the same SA intensity normalization as in Table II is used in these Tables and in all further discussion. As shown in the ESI†, the intensities for I>.0001 are almost exactly the same as the totals that include all ionic states. For each threshold, the count of the number of states that contribute to the I_{rel} summations is also given. There are two purposes to this comparison. One is to show the quantitative importance of $2p_{1/2}$ and $2p_{3/2}$ contributions to the intensity of the different regions. The second is to show that the intensity does not arise from only a few ionic states but that there are contributions, usually unresolved, from literally 100s of different ionic states. The 2p XPS is not simply a one-electron process.

Region (1): 0.0≤BE(rel)<6.0 eV

For the SO WFs in the first region, the SA XPS intensity, see Table III, is almost entirely from Fe $2p_{3/2}$ ionization with only 2% of the intensity arising from $2p_{1/2}$ ionization. The dominance of the Fe $2p_{3/2}$ ionization can also be seen from Fig. 2. The intensity in this region is a large fraction, 63% of the total Fe 2p XPS intensity with the SO WFs; see Fig. 3(a). However, for I>.0001, 251 different states contribute to $I_{rel}(2p)$. These states arise because of small spin-orbit and ligand field splittings of the 3d electrons. When the threshold for including contributions of individual states to the sum is increased by a factor of 50 to I>0.005, the 129 states at this threshold still contribute more than 98% of the total intensity in this region. The intensities in

this region for the CI14 WFs, as shown in Table IV are quite similar, although they are distributed over a larger number of states. The similarity of the results for the SO and CI14 WFs are compelling evidence that shake excitations make only a minor contribution to the XPS intensity in this region. Thus, the main origin of the XPS in this region is the angular momentum coupling of different multiplets with the KC configuration.

Region 2: 6.0≤BE(rel)<12.0 eV

For the SO WFs in region 2, while there are a large number, 568, of states with I>0.0001, the total intensity is small, ~12% of the $I_{rel}(2p)$ in region 1 and largely from $2p_{3/2}$ ionization; see Table III. For the CI14 WFs, see Table IV, the total intensity is much larger, almost 50% of the intensity in region 1 and the intensity from ionization of $2p_{3/2}$ is 89% of the total. This is a strong indication that this region has shake excitations from closed shell O(2p) to the open shell, dominantly Fe(3d), orbitals. This will be demonstrated in more detail in the following section. If one increases the threshold by a factor of 10, one still has over 95% of the total intensity but still with almost 80% of the total number of states. When the threshold is further increased to I>0.005, one has many fewer states, only 355, and the intensity is reduced by a very large amount, over one third. These are clear indications that the intensity in this region is distributed over more than 1,000 states, each with only a small intensity. The many states are now formed from the angular momentum coupling of small spin-orbit and ligand field splittings of the open shell orbitals but now there will also be excitations from the closed shell O(2p) γ_8 orbital into the Fe 3d open shell space. The composition of these states is examined in more detail in the following section.

Region 3: 12.0≤BE(rel)<18.0 eV

From Table III for the SO WFs in region 3, there are 230 states with I>0.0001 and 95% of the intensity is from $2p_{1/2}$ ionization with a total intensity, $I_{rel}(2p)$ that is almost half of the intensity in region 1. This is expected from the statistical ratio of the $2p_{1/2}$ and $2p_{3/2}$ occupations; see, for example Ref. [11]. Furthermore, over 97% of the intensity comes from the 136 states with I>0.005. However, we show in Sec. V that the composition of the states in this region does not arise simply from the angular momentum coupling of an open shell $2p_{1/2}$ electron with the open valence shell, dominantly 3d, electrons. The data in Table IV shows that the situation for this region changes significantly when shake excitations are allowed and the CI14 WFs are used. The total intensity, for states with I>0.0001, increases by almost 20% over the intensity in this region for the SO WFs mainly from an increase of the CI14 $I_{rel}(2p_{3/2})$. Furthermore, if one takes into account only the states with I>0.005, one obtains only 70% of the intensity in this region; a compelling indication that the intensity arises from well over 1,000 states with low intensity.

Region 4: 18.0≤BE(rel)<26.0 eV

For the SO WFs in the fourth region, Table III shows that there is very little intensity, less than 3% of the total SO SA intensity, as given in Table II, and mostly, 85%, from $2p_{1/2}$ ionization. Once shake is included, Table IV, the intensity increases to 11% of the total CI14 SA intensity; this increase is consistent with the intensity of the measured XPS satellite at ~23 eV; see Fig. 1(b). The $2p_{1/2}$ ionizations are responsible for 88% of the total intensity and it is tempting to assign this region to shake excitations arising from $2p_{1/2}$ ionization but this is somewhat of an oversimplification as shown in the following section. Furthermore, large fractions of the total intensity are lost if only the intensities from states with I>0.001 or I>0.005 are considered.

V. Composition of States in the Different Regions

As we have seen in Sec. IV, there are a very large number of states in these regions and it is not possible to examine the properties of individual states. Thus, we divide the regions into groups of states with BEs in a range of 0.5 eV. Thus, for the first region, there would be 12 such groups with the lowest BE group being for states with $0 \leq BE(rel) < 0.5$ eV and the highest BE group being for states with $5.5 \leq BE(rel) < 6$ eV. There are analogous groups of states for the other three regions. For each group, properties of the states in the group are shown graphically in Figs. 4(a) for the SO WFs and 4(b) for the CI14 WFs. Tabulations of the properties of the states in the groups are given in the ESI† in Tables SII-SV; graphical features of the properties of the groups in individual regions are given in the ESI† in Figs. S1 to S4. While the overall features of the groups are shown in Fig. 4, the tables and figures in the ESI† allow the interested reader to determine finer details for the different groups of states. In Fig. 4, the properties of states in the Group from $E_i \leq BE(rel) < E_i + 0.5$ eV are shown above the energy $E_i + 0.5$ In the figures, the experimental data is also plotted and aligned to BE(rel) as in Figs. 1. The following three groups of data are presented:

(1) The SA I_{rel} summed over all the states in a group, is given as a vertical bar in the figures. The same SA intensity normalization as used in Tables II-IV is also used here. Since the same normalization is used for the intensity bars for all regions, the relative intensities in the different groups and regions can be directly compared. In addition, these vertical bars can be compared with the experimental curve which is also shown in Fig. 4; however, care should be taken since the bars are not broadened to account for experimental resolution and core-hole lifetime.

(2) The average occupations of the $2p_{3/2}$ and $2p_{1/2}$ shells for the states in the group are shown in the figures as red ($2p_{3/2}$) and blue ($2p_{1/2}$) dots and in the SI tables as Occ($2p_{3/2}$) and Occ($2p_{1/2}$). The occupation numbers for an individual final state are simply the expectation values of the number operators for the orbitals; see, for example Ref.[60]. The group averages are the occupation number of a state multiplied by its XPS SA intensity summed over all the states in the group and normalized by the total intensity of the states in the group.

(3) For the CI14 WFs, there is an additional occupation which is used to provide an estimate of the shake excitations. This quantity, shown in Fig. 4(b) as a green dot and denoted in the ESI† tables as Occ(Shake), is (4-Occ[active O]), where 4 is the full occupation of the active orbitals of dominantly O(2p) character, see Table I. The reduction of occupation of these active orbitals from 4, with a corresponding increase in the occupation of the active orbitals of 3d character, see Table I, indicates an increase in the shake character of a state. The values of shake occupation are intensity weighted averages as for the $2p_{3/2}$ and $2p_{1/2}$ occupations. The shake occupation will be greater than zero even for the lowest lying states because of the many-electron character of the WFs which cannot be described by a single configuration. [11, 17, 61] However, the variation of the values of the shake occupation for the different groups and different regions and the connection of Occ(Shake) to the XPS intensity will indicate the extent that we can use the shake character to distinguish among different features in an XPS spectra.

In the following discussion, the properties of the states for the SO WFs and the CI14 WFs are compared and the characteristics of the states in the different regions are contrasted. While the discussions on these properties are organized around the states in each region separately, Fig. 4 which includes the groups in all regions shows the trends of intensities and occupations across the entire energy range of the Fe 2p XPS.:

Region 1, 0≤BE(rel)<6.0 eV

If the ionization in the WF were entirely from $2p_{3/2}$, then the $2p_{1/2}$ occupation would be 2 and the $2p_{3/2}$ occupation would be 3 since an electron is removed from this subshell. It is clear from Fig. 4, that in Region 1 these occupations, for both the SO and CI14 WFs, are very close to these ideal values. This is fully consistent with the data in Fig. 3 and Tables III and IV and proves that the conventional assignment of this feature [29, 58-59] is correct. For the SO WFs in this Region, most of the intensity is in two groups separated by 1.0 eV which is consistent with the doublet observed both in the calculation and the XPS measurement. For the CI14 WFs, where shake is included, Fig. 4(b), the largest intensity is still for the first group with 0≤BE(rel)<0.5 eV but the remaining intensity is distributed over more groups than for the SO WFs. For the CI14 WFs, there is also a small to modest contribution from the shake occupations; see the discussion in the ESI†. Overall, these small shake contributions are not sufficiently large to consider the states in this region as having significant shake character. The minor importance of shake configurations in this region is confirmed by the strong similarity of the results for the SO WFs and the CI14 WFs, see Fig. 1.

Region 2, 6.0≤BE(rel)<12.0 eV

As we have noted earlier, see Table III, the Fe 2p XPS intensity in this region for the SO WFs is small and dominated by $2p_{3/2}$ ionization. This is consistent with the $2p_{3/2}$ occupations of ≈3 shown in Fig. 4 and Table SII. For the much larger Fe 2p XPS SA intensity obtained with the CI14 WFs, the data shows that the $2p_{3/2}$ and $2p_{1/2}$ occupations still largely have the ideal values for $2p_{3/2}$ ionization. However now that the shake occupations are included, the intensity in this region is large, being 49% of the intensity in Region 1, see Table IV. It is reasonable to argue

that the intensity in this region arises because shake excitations are allowed. Most of the intensity in this region is in five groups at group energies of 9.5 and 10.5 to 12.0 eV; see Fig. 4(b). In these regions, the Occ(Shake) is between 0.85 and 0.87, see Table SIII, which is larger than the largest Occ(Shake) in Region 1. Thus, while a large shake character does not, in itself, assure that there will be a large XPS intensity, see the group for 4.0≤BE(rel)<4.5 eV in Region 1, it does seem that satellites with large XPS intensity will also have a large shake character. This provides the first *ab initio* support for the character of this region as a shake satellite for the Fe $2p_{3/2}$ ionization.

Region 3, 12.0≤BE(rel)<18.0 eV

The properties of the states in Region 3, see Fig. 4 and Table SIV, are quite different from those in the preceding two regions. We consider first an unexpected property of the SO WFs. While the intensity for the SO WFs in this region is 95%, from $2p_{1/2}$ ionization, the $2p_j$ occupations do not have the ideal values of Occ($2p_{1/2}$)=1 and Occ($2p_{3/2}$)=4. For the group at 15.5≤BE(rel)<16.0 eV, which has almost the maximum SA intensity, the Occ($2p_{1/2}$) is 1.3 while for the group with the highest SA intensity, at 14.0≤BE(rel)<14.5 eV, the Occ($2p_{1/2}$) is 1.6; both of these values of Occ($2p_{1/2}$) are significantly larger than 1. A value of Occ($2p_{1/2}$)=1.6 for a group indicates that the configurations with slightly over half of the weights for the WFs in this group have a 2p occupation of $(2p_{1/2})^2(2p_{3/2})^3$ rather than the expected $(2p_{1/2})^1(2p_{3/2})^4$ occupation. It would appear to be a contradiction that there is very little intensity in this group from Fe($2p_{3/2}$) ionization while the states in the group have major contributions from configurations where an electron is removed from the $2p_{3/2}$ subshell rather than from the $2p_{1/2}$ shell. Our earlier work on the analysis of the Ti 2p XPS in TiO_2 and STO, both nominally closed shell Ti(IV) compounds

[55] identifies the essential physics that resolves the apparent contradiction. Here we extend the logic of Ref. [55] to Fe_2O_3. The six nearly degenerate initial states of Fe_2O_3 can be viewed as having the open d shell coupling of $d^5(^6S)$. States where the d electrons are recoupled to different multiplets will have higher energy than the ^6S coupling. [50, 62] These recoupled d shell electrons can couple with a $2p^5$ occupation of $(2p_{1/2})^2(2p_{3/2})^3$ which will be in the same energy range as $d^5(^6S)$ coupled with a $(2p_{1/2})^1(2p_{3/2})^4$. However, the former configurations are XPS forbidden while the latter configurations are XPS allowed. Since the two sets of configurations have comparable diagonal energies, there could be strong mixing of the XPS allowed and forbidden configurations. It can be seen from the occupations of the SO WFs that this mixing is considerable and leads to many ionic states with significant XPS intensity from $2p_{1/2}$ ionization but also with significant contribution from XPS forbidden configurations with $(2p_{1/2})^2(2p_{3/2})^3$ 2p shell character. In other words, even without considering shake excitations, the states in this region have considerable multiconfigurational character. When shake excitations are added, the multiconfigurational character becomes more complex.

The data in Tables III and IV show that, for the CI14 WFs, the total intensity in this region increases by ~20% over the intensity for the SO WFs and is now 55% of the CI14 WF intensity in Region 1, close to the statistical ratio from the $2p_{1/2}$ and $2p_{3/2}$ occupations. The ratio of 55% is not surprising since the SA intensity here is dominated by contributions from $2p_{1/2}$ ionization while that in Region 1 is due to $2p_{3/2}$ ionization. Furthermore, 80% of the intensity is distributed almost uniformly over the six groups from $13.5 \leq BE(rel) < 16.5$eV. The involvement of configurations with 2p occupations of $(2p_{1/2})^2(2p_{3/2})^3$ is rather large as can be seen from Fig. 4(b) and Table SIV. In this region, the values of $Occ(2p_{1/2})$ and $Occ(2p_{3/2})$ are very far from those expected for WFs dominated by configurations with $(2p_{1/2})^1(2p_{3/2})^4$ In addition, the shake

occupations for the groups in this region are large, comparable to, but slightly larger those obtained for Region 2. In other words, the states in this region have considerable shake character.

Region 4, 18.0≤BE(rel)<26.0 eV

The intensity for the SO WFs in this region is small, less than 10% of the intensity in Region 3; see Table III. It is not discussed further. When shake excitations with the CI14 WFs are included, the total intensity in this region increases to become 50% of the intensity in Region 3 and it is almost entirely from contributions from $2p_{1/2}$ ionization; see Table IV. However, the CI14 WFs in this group have $2p_{1/2}$ occupations with Occ($2p_{1/2}$) about 1.6, indicating that configurations with 2p shell occupations of $(2p_{1/2})^2(2p_{3/2})^3$ form more than half the weight of these states; see Fig. 4(b) and Table SV. Moreover, the shake occupations are considerably larger here than in Region 3; for the two groups with the largest intensity, the shake occupation is ~1.5 indicating a very large shake character of the states in this region. Overall, the states in Regions 3 and 4 that have major Fe 2p XPS intensity have large shake character with the shake character in Region 4 being considerably larger than for Region 3.

VI. Conclusions

A detailed *ab initio* analysis of the character of the main peaks and the satellites has been made using a new approach to forming an orbital set that will have approximately equal accuracy for the "main" and "satellite" features. With this orbital set we have been able to reproduce most of the intrinsic features of the Fe 2p XPS of Fe_2O_3 with modest accuracy with an *ab initio* methodology where parameters are not selected based on finding agreement between theory and experiment. A special value our analysis is that it can provide guidance for the selection of parameters that are used in empirical fits to the Fe 2p XPS of Fe_2O_3 as used, for example, by

Sanchez *et al.* [63] and many people before that. We have also been able to rigorously separate the XPS intensity due to ionization of the Fe $2p_{1/2}$ and $2p_{3/2}$ electrons. In addition, we have determined the occupations of the $2p_{1/2}$ and $2p_{3/2}$ orbitals in the different ionic WFs. A simple view is that the final states that have large $2p_{3/2}$ XPS intensity should have occupations that are close to $Occ(2p_{3/2})=3$ and $Occ(2p_{1/2})=2$ and those with a large $2p_{1/2}$ XPS intensity would have occupations that are close to $Occ(2p_{3/2})=4$ and $Occ(2p_{1/2})=1$. This is expected since these occupations correspond to the ideal ionization of either the $2p_{3/2}$ or the $2p_{1/2}$ shells. However, we have found that this simple view does not hold. The many body effects are sufficiently important that the 2p sub-shell occupations in the ionic WFs do not even nearly reflect the XPS intensity. This is a direct reflection of the many-body character of the ionic states where the XPS allowed and the XPS forbidden configurations are mixed over literally hundreds of states.

With the analysis of the XPS predicted from our WFs, we have been able to reach several new and important conclusions concerning the interpretation and use of the XPS data for Fe_2O_3 and, by extension, probably for other ionic compounds, although this general validity is not certain without verification. We have shown that XPS intensity in different regions of the XPS usually arises from the sum of small intensities from tens to hundreds, if not thousands, of individual states. For the XPS of Fe(III). this represents a major extension of the work of Gupta and Sen [3] who examined only the angular momentum coupling of the open atomic 2p and 3d shell. They did not take into account the covalent character and ligand field splitting of the orbitals as well as the contributions of shake configurations. It is these terms that lead to the broad distribution of intensity that we have shown. In particular, we have shown that it is not always possible to associate features in the XPS to a single or to a few ionic states. It is common that there are cases where the states are nearly degenerate with small energy splittings arising

from spin-orbit and ligand field splittings as well as mixings from configurations with different occupations of orbitals in the active orbital space. This active space includes the open valence and core shell orbitals as well as orbitals needed to describe shake excitations. These latter orbitals are dominantly ligand orbitals that have significant covalent bonding character between ligand and cation. The degeneracies of the ionic states are usually too small to be resolved because of the XPS energy resolution and core-hole lifetime broadening. In order to analyze the electronic character, we divided the BEs into regions that have been commonly associated with "main" and "satellite" features arising from $2p_{3/2}$ and $2p_{1/2}$ ionization. Because of the large number of different states, we have shown the value of dividing the XPS in these different regions into groups within a small, 0.5 eV, energy range and examined the average character of the states in each of these groups. The properties of the states in the different groups are different from each other and in some cases different from the assignments that are usually made.

For the first region, $0.0 \leq BE(rel) < 6.0$ eV, the intensity is close to that expected for ionic multiplets arising simply from the angular momentum coupling of the $2p_{3/2}$ shell with the open valence shell of five dominantly d electrons. In particular, shake configurations do not make large contributions to the WFs in this region. This is not at all the case for the second region, $6.0 \leq BE(rel) < 12.0$. The intensity in this region can be described as arising from $2p_{3/2}$ ions where there is also a shake excitation from dominantly O(2p) bonding orbitals into the open dominantly Fe 3d orbitals. Moreover, this intensity is distributed over an unexpectedly large number of states. While this interpretation largely agrees with the usual assignments for these features, this is the first time, to our knowledge, that *ab initio* methods have confirmed these assignments.

The situation is very different for the third, $12.0 \leq BE(rel) > 18.0$ eV, and fourth, $18.0 \leq BE(rel) < 26$ eV, regions. The WFs in the third region do not have the $2p_j$ occupations that

follow from the $2p_{1/2}$ shell being singly occupied and the $2p_{3/2}$ shell being filled. Rather the weights in these WFs of an electron being removed from the $2p_{3/2}$ sub-shells is significantly larger than the weight of an electron being removed from the $2p_{1/2}$ shell. This even though the intensity in this region due to $2p_{1/2}$ ionization accounts for 80% of the total intensity in the region with only 20% due to $2p_{3/2}$ ionization. The apparent contradiction is resolved by understanding the WFs in this region are strong mixtures of XPS forbidden configurations that have $(2p_{1/2})^2(2p_{3/2})^3$ occupations while the XPS allowed configurations usually have $(2p_{1/2})^1(2p_{3/2})^4$ occupations. Furthermore, the WFs in this third region have significant shake character. The combination of these two many body features leads to a somewhat uniform distribution of intensity over the states in a range of ~ 3 eV. Similar remarks can be made for the "satellite" Region 4 where there is an even larger contribution from shake occupations than in Region 3. The conclusion is that Region 3 cannot be described as main $2p_{1/2}$ feature nor can Region 4 be described as a shake or CT satellite. The states in both regions are combinations of configurations with different $2p_j$ occupations and with significant shake character. However, it is necessary to stress that while a large Occ(shake) and, hence, a large shake character is a property necessary for satellites to have significant intensity, it is not, in itself, sufficient to ensure that a state in a satellite region will have a large intensity. This is another demonstration of the many-electron, many-configuration, character of the states where XPS allowed and XPS forbidden configurations may mix strongly in the excited states.

The difference between the character of the states in these regions indicates that it is only Region 1 where one can assign unresolved or partly resolved individual final states very largely to the angular momentum coupling of the open core and valence level open shell electrons. This

form of analysis was originally proposed in the pioneering work of Gupta and Sen [2-3] for 3d transition metal compounds. Our results indicate that such a multiplet analysis, while appropriate for Region 1, is not appropriate for the other regions of the 2p XPS.

A different, but also rather important, result of our analysis concerns the extent of the losses of XPS intensity to features due to states not included in our theoretical analysis. For the SO WFs, where shake satellites are not included, 40% of the Fe 3p XPS intensity is lost to satellites that have shake character. However, for the CI14 WFs where shake satellites are included, the losses to satellites not included is only 12%. Furthermore, the 88% of the total XPS intensity that is recovered with the CI14 WFs is within a range of BEs that is not especially large and one which is commonly included in XPS measurements; specifically, it is within BE(rel)≤35 eV, see Fig. 3(b). If this kind of information were available for other oxides, it would be useful in providing a stronger foundation for estimating stoichiometry [64] and for evaluating the reliability of the subtractions used to remove background. [29, 56-57]

The use of fractional occupations for the variational determination of orbitals to be used to study both main and satellite XPS features developed for this study could also be appropriate to be used to determine the satellite features of other compounds. While the present work is restricted to the analysis of the main and satellite features of Fe_2O_3, the extension of this study to oxide compounds with different oxidation states and different geometries could be a major aid in extracting information form their XPS. This should be true both for insight into the properties of the initial, unionized, and final, ionized states and for the practical analysis to determine stoichiometries and to distinguish the properties of bulk atoms from those of surface atoms.

Conflicts of interest

There are no conflicts of interest to declare

Acknowledgements

This material is based upon work supported by the U.S. Department of Energy, Office of Science, Office of Basic Energy Sciences, Chemical Sciences, Geosciences, and Biosciences (CSGB) Division through its Geosciences program at Pacific Northwest National Laboratory (PNNL). PNNL is a multi-program national laboratory operated for the DOE by Battelle Memorial Institute under contract no. DE-AC05-76RL01830.

Table I. Orbital character and properties of selected orbitals from DHF calculations on three configurations of Fe_2O_3 denoted: SO – initial, SO – 2p Ion, and CI14 – 2p Ion where relevant shell occupations are shown. The orbitals are grouped into nearly degenerate sets where the O_h relativistic and non-relativistic symmetries and degeneracies are given. The relative orbital energies, ε(rel), effective size, r_{eff}, and projected Fe 3d character, $N_P(3d)$, are averaged over the nearly degenerate sets. See text for details.

SO-Initial with $Fe(2p)^6O(2p)^{36}Fe(3d)^5$				
Orbital-(number)	O_h Symmetry	ε(rel)-eV	r_{eff} – Å	$N_P(3d)$
O(2p)-(4)	γ_8	0.00	2.10	0.06
O(2p)-(4)	γ_8	1.21	2.13	0.05
O(2p)-(2)	γ_7	3.82	2.23	0.03
Fe(3d)-(4)	$\gamma_8[t_{2g}]$	8.96	0.70	0.96
Fe(3d)-(2)	$\gamma_7[t_{2g}]$	9.04	0.70	0.96
Fe(3d)-(4)	$\gamma_8[e_g]$	10.31	0.90	0.84
SO-2p Ion with $Fe(2p)^5O(2p)^{36}Fe(3d)^5$				
Orbital-(number)	O_h Symmetry	ε(rel)-eV	r_{eff} – Å	$N_P(3d)$
O(2p)-(4)	γ_8	0.00	1.78	0.46
Fe(3d)-(4)	$\gamma_8[t_{2g}]$	5.13	0.77	0.92
Fe(3d)-(2)	$\gamma_7[t_{2g}]$	5.31	0.79	0.90
Fe(3d)-(4)	$\gamma_8[e_g]$	7.39	1.53	0.46
CI14-2p Ion with $Fe(2p)^5O(2p)^{35.5}Fe(3d)^{5.5}$				
Orbital-(number)	O_h Symmetry	ε(rel)-eV	r_{eff} – Å	$N_P(3d)$
O(2p)-(4)	γ_8	0.00	2.07	0.19
Fe(3d)-(4)	$\gamma_8[t_{2g}]$	4.27	0.72	0.93
Fe(3d)-(2)	$\gamma_7[t_{2g}]$	4.40	0.73	0.93
Fe(3d)-(4)	$\gamma_8[e_g]$	6.42	1.19	0.66

Table II. Summed SA Intensities for the Fe 2p XPS of Fe_2O_3 over the SO final states and over the CI14 final states. The XPS intensities into all possible final states, Complete final states, are given to show the SA normalization used. The percent losses for the SO and CI14 final states are also given. The intensities are separated into $I_{rel}(2p_{1/2})$, $I_{rel}(2p_{1/2})$, and $I_{rel}(2p)$.

	$I_{rel}(2p_{1/2})$	$I_{rel}(2p_{3/2})$	$I_{rel}(2p)$
Complete	12.00	23.99	35.99
SO	7.19	14.38	21.57
SO Losses[a]	40.1%	40.1%	40.1%
CI14	10.56	21.12	31.69
CI14 Losses[a]	12.0%	12.0%	12.0%

[a]These losses of intensity may be to BEs within the energy range of Fig. 1 or they may be to BEs larger than this energy range.

Table III. Distribution of SA intensities for the SO WFs in the four different BE(rel) regions of the Fe 2p XPS of Fe_2O_3. For each region, the summed SA intensities, I_{rel}, are given for $2p_{1/2}$ and $2p_{3/2}$ and for the sum of the two ionizations. These intensities are given for sums taken with three thresholds: (1) sums of intensities for ionic states with total intensity I>0.0001; (2) sums over sates with I>0.001 and (3) sums over states with I>0.005. For each of these thresholds, the count of the number of states with intensities within the thresholds are also given. The fraction of the state count and intensity for the I>0.001 and I>0.005 thresholds are given as a percent. See text for further details

Region - eV	Threshold	Count	$I_{rel}(2p_{1/2})$	$I_{rel}(2p3_{/2})$	$I_{rel}(2p)$
0.0≤BE<6.0	I>0.0001	251	0.31	12.85	13.16
	I>0.001	223(88.8%)	0.31(98.3%)	12.83(99.9%)	13.14(99.9%)
	I>0.005	129(51.4%)	0.26(83.4%)	12.68(98.7%)	12.93(98.3%)
6.0≤BE<12.0	I>0.0001	568	0.46	1.16	1.62
	I>0.001	398(70.1%)	0.41(89.6%)	1.13(97.5%)	1.54(95.3%)
	I>0.005	136(23.9%)	0.18(39.1%)	0.89(76.5%)	1.06(65.9%)
12.0≤BE<18.0	I>0.0001	230	5.93	0.30	6.24
	I>0.001	170(73.9%)	5.91(99.6%)	0.30(99.3%)	6.21(99.6%)
	I>0.005	102(44.3%)	5.97(97.6%)	0.29(95.6%)	6.08(97.5%)
18.0≤BE<26.0	I>0.0001	311	0.49	0.08	0.56
	I>0.001	150(48.2%)	0.45(92.3%)	0.06(83.5%)	0.51(91.1%)
	I>0.005	39(12.5%)	0.31(63.3%)	0.03(44.5%)	0.34(60.7%)

.

Table IV. Distribution of SA intensities for the CI14 WFs in the four different BE(rel) regions of the Fe 2p XPS of Fe_2O_3. See caption to Table IV and text details

Region - eV	Threshold	Count	$I_{rel}(2p_{1/2})$	$I_{rel}(2p3_{/2})$	$I_{rel}(2p)$
0.0≤BE<6.0	I>0.0001	493	0.31	13.20	13.51
	I>0.001	459(91.3%)	0.30(98.7%)	13.18(98.7%)	13.48(99.8%)
	I>0.005	237(48.1%)	0.23(75.5%)	12.70(96.2%)	12.93(95.7%)
6.0≤BE<12.0	I>0.0001	1922	0.70	5.91	6.61
	I>0.001	1493(77.7%)	0.62(88.9%)	5.71(96.6%)	6.33(95.8%)
	I>0.005	355(18.5%)	0.18(26.1%)	4.00(67.7%)	4.18(63.3%)
12.0≤BE<18.0	I>0.0001	1633	5.88	1.49	7.37
	I>0.001	1460(87.8%)	5.81(98.8%)	1.43(96.1%)	7.24(98.2%)
	I>0.005	587(35.3%)	4.57(77.7%)	0.80(53.6%)	5.37(72.8%)
18.0≤BE<26.0	I>0.0001	3262	3.25	0.45	3.70
	I>0.001	582(17.8%)	1.99(61.0%)	0.19(43.2%)	2.18(58.8%)
	I>0.005	116(3.5%)	0.91(28.0%)	0.07(14.6%)	0.98(26.4%)

.

References

1. P. S. Bagus, A. J. Freeman, and F. Sasaki, Phys. Rev. Lett., 1973, **30**, 850-853.
2. R. P. Gupta and S. K. Sen, Phys. Rev. B, 1974, **10**, 71-77.
3. R. P. Gupta and S. K. Sen, Phys. Rev. B, 1975, **12**, 15-19.
4. E.-K. Viinikka and Y. Öhrn, Phys. Rev. B, 1975, **11**, 4168.
5. J. Zaanen, C. Westra, and G. A. Sawatzky, Phys. Rev. B, 1986, **33**, 8060-8073.
6. J. Zaanen and G. A. Sawatzky, Prog. Theor. Phys. Suppl., 1990, 231-270.
7. K. Okada, A. Kotani, and B. T. Thole, J. Electron Spectrosc. Relat. Phenom., 1992, **58**, 325-343.
8. K. Okada and A. Kotani, J. Phys. Soc. Jpn., 1992, **61**, 4619-4637.
9. F. De Groot and A. Kotani, *Core level spectroscopy of solids. CRC Press, Boca Raton*, 2008).
10. P. S. Bagus, E. S. Ilton, and C. J. Nelin, Surf. Sci. Rep., 2013, **68**, 273.
11. P. S. Bagus, E. S. Ilton, and C. J. Nelin, Catal. Lett., 2018, **148**, 1785-1802.
12. P. S. Bagus, C. J. Nelin, and E. S. Ilton, J. Chem. Phys., 2013, **139**, 244704.
13. S. A. Chambers, M. H. Engelhard, L. Wang, T. C. Droubay, M. E. Bowden, M. J. Wahila, N. F. Quackenbush, L. F. J. Piper, T.-L. Lee, C. J. Nelin, and P. S. Bagus, Phys. Rev. B, 2017, **96**, 205143.
14. T. Aberg, Phys. Rev., 1967, **156**, 35.
15. R. Manne and T. Åberg, Chem. Phys. Lett., 1970, **7**, 282.
16. P. S. Bagus, C. J. Nelin, D. A. Hrovat, and E. S. Ilton, J. Chem. Phys., 2017, **146**, 134706.
17. P. S. Bagus, C. J. Nelin, C. R. Brundle, N. Lahiri, E. S. Ilton, and K. M. Rosso, J. Chem. Phys., 2020, **152**, 014704.
18. J. J. Kas, J. J. Rehr, and T. P. Devereaux, arXiv:2107.10409v1, 2021.
19. S. I. Bokarev and O. Kühn, WIREs Computational Molecular Science, 2020, **10**, e1433.
20. P. Norman and A. Dreuw, Chem. Rev., 2018, **118**, 7208-7248.
21. D. Golze, J. Wilhelm, M. J. van Setten, and P. Rinke, J. Chem. Theory Comput., 2018, **14**, 4856-4869.
22. D. Golze, L. Keller, and P. Rinke, J, Phys. Chem. Lett, 2020, **11**, 1840-1847.
23. P. W. Langhoff, S. R. Langhoff, T. N. Rescigno, J. Scirmer, L. S. Cederbaum, W. Domcke, and W. Von Niessen, Chem. Phys., 1981, **58**, 71-91.
24. F. Viñes, C. Sousa, and F. Illas, Phys. Chem. Chem. Phys., 2018, **20**, 8403-8410.
25. J. J. Rehr and J. J. Kas, J. Vac. Sci. Technol., A, 2021, **39**, 060401.
26. P. S. Bagus, C. J. Nelin, C. R. Brundle, B. V. Crist, N. Lahiri, and K. M. Rosso, J. Chem. Phys., 2020, **153**, 194702.
27. I. N. Levine, *Quantum Chemistry* (Prentice-Hall, Upper Saddle River, NJ, 2000).
28. P. S. Bagus, M. J. Sassi, and K. M. Rosso, J. Chem. Phys., 2019, **151**, 044107.
29. P. S. Bagus, C. J. Nelin, C. R. Brundle, B. V. Crist, N. Lahiri, and K. M. Rosso, J. Chem. Phys., 2021, **154**, 094709.
30. T. Koopmans, Physica 1934, **1**, 104.
31. N. P. Bellafont, F. Illas, and P. S. Bagus, Phys. Chem. Chem. Phys., 2015, **17**, 4015.
32. P. S. Bagus and F. Illas, Catal. Lett., 2020, **150**, 2457.
33. P. S. Bagus, C. Sousa, and F. Illas, J. Chem. Phys., 2016, **145**, 144303.
34. C. S. Fadley, "Basic Concepts of X-Ray Photoelectron Spectroscopy", in *Electron Spectroscopy: Theory, Techniques and Applications*, edited by C. R. Brundle and A. D. Baker (Academic Press, 1978), Vol. 2, p. 2-145.
35. K. Okada, A. Kotani, and B. T. Thole, J. Electron Spectrosc. Relat. Phenom., 1992, **58**, 325-343.
36. T. Saue, R. Bast, A. S. P. Gomes, H. J. A. Jensen, L. Visscher, I. A. Aucar, R. D. Remigio, K. G. Dyall, E. Eliav, E. Fasshauer, T. Fleig, L. Halbert, E. D. Hedegård, B. Helmich-Paris, M. Iliaš, C. R. Jacob, S.

Knecht, J. K. Laerdahl, M. L. Vidal, M. K. Nayak, M. Olejniczak, J. M. H. Olsen, M. Pernpointner, B. Senjean, A. Shee, A. Sunaga, and J. N. P. v. Stralen, J. Chem. Phys., 2020, **152**, 204104.
37. R. S. Mulliken, J. Chem. Phys., 1955, **23**, 1833-1840.
38. R. S. Mulliken, J. Chem. Phys., 1955, **23**, 1841-1846.
39. R. S. Mulliken, J. Chem. Phys., 1955, **23**, 2338-2342.
40. R. S. Mulliken, J. Chem. Phys., 1955, **23**, 2343-2346.
41. J. Hernandez-Trujillo and R. F. W. Bader, J. Phys. Chem. A, 2000, **104**, 1779-1794.
42. A. E. Reed, R. B. Weinstock, and F. Weinhold, J. Chem. Phys., 1985, **83**, 735-746.
43. P. S. Bagus and C. J. Nelin, J. Electron Spectrosc. Relat. Phenom., 2014, **194**, 37.
44. C. J. Ballhausen, *Introduction to Ligand Field Theory* (McGraw-Hill, New York, 1962).
45. J. A. Gubner, J. Phys. A, 1994, **27**, L745-749.
46. P. S. Bagus and C. J. Nelin, "Computation of Vibrational Excitations in XPS Spectroscopy", in *Rare Earth Elements and Actinides: Progress in Computational Science Applications*, edited by D. A. Penchoff, et al. (American Chemical Society, 2021), Vol. 1388, p. 181.
47. *DIRAC, a relativistic ab initio electronic structure program, Release DIRAC08 (2008), written by L. Visscher, H. J. Aa. Jensen, and T. Saue, with new contributions from R. Bast, S. Dubillard, K. G. Dyall, U. Ekström, E. Eliav, T. Fleig, A. S. P. Gomes, T. U. Helgaker, J. Henriksson, M. Iliaš, Ch. R. Jacob, S. Knecht, P. Norman, J. Olsen, M. Pernpointner, K. Ruud, P. Sałek, and J. Sikkema (see the URL at http://dirac.chem.sdu.dk.* .
48. P. O. Löwdin, Phys. Rev., 1955, **97**, 1474-1489.
49. F. Prosser and S. Hagstrom, Int. J. Quantum Chem., 1968, **2**, 89-99.
50. J. S. Griffith, *The Theory of Transition-Metal Ions* (Cambridge Press, Cambridge, 1971).
51. S. L. Altmann and P. Herzig, *Point-Group Theory Tables* (Clarendon Press, Oxford, 1994).
52. C. J. Nelin, P. S. Bagus, E. S. Ilton, S. A. Chambers, H. Kuhlenbeck, and H. J. Freund, Int. J. Quantum Chem., 2010, **110**, 2752-2764.
53. C. R. Brundle, T. J. Chuang, and K. Wandelt, Surf. Sci., 1977, **68**, 459-468.
54. T. Yamashita and P. Hayes, Appl. Surf. Sci., 2008, **254**, 2441-2449.
55. P. S. Bagus, C. J. Nelin, C. R. Brundle, and S. A. Chambers, J. Phys. Chem. C, 2019, **123**, 7705-7716.
56. C. R. Brundle, B. V. Crist, and P. S. Bagus, J. Vac. Sci. Technol., A, 2021, **39**, 013202.
57. P. S. Bagus, C. R. Brundle, and B. V. Crist, J. Vac. Sci. Technol., A, 2021, **39**, In press.
58. A. P. Grosvenor, B. A. Kobe, M. C. Biesinger, and N. S. McIntyre, Surf. Interface Anal., 2004, **36**, 1564-1574.
59. M. C. Biesinger, B. P. Payne, A. P. Grosvenor, L. W. M. Lau, A. R. Gerson, and R. S. C. Smart, Appl. Surf. Sci., 2011, **257**, 2717-2730.
60. L. D. Landau and E. M. Lifshitz, *Quantum Mechanics* (Addison-Wesley, Reading, 1958).
61. P. S. Bagus, B. Schacherl, and T. Vitova, Inorg. Chem., 2021.
62. C. E. Moore, *Atomic Energy Levels, Natl. Bur. Stand. No. 467, U. S. GPO, Washington, D. C. 1952; see also, URL http://physics.nist.gov/cgi-bin/AtData/main_asd.*
63. M. B. Sanchez, J. A. Huerta-Ruelas, D. Cabrera-German, and A. Herrera-Gomez, Surf. Interface Anal., 2017, **49**, 253-260.
64. C. R. Brundle and B. V. Crist, J. Vac. Sci. Technol., A, 2020, **38**, 041001.

Figure Captions

Fig. 1. Plots of the theoretical predictions for the Fe 2p XPS of Fe_2O_3, with solid curves, compared to experiment, dotted curve: (a) for SO ionic states where only angular momentum is treated and (b) for CI14 ionic states where shake configurations are included. The total predicted XPS is a bold line and large individual contribution for specific final states are in lighter curves, color online. See text for details.

Fig. 2. Plot of the theoretical predictions for the $2p_{1/2}$, dashed blue line, and the $2p_{3/2}$, dashed red line, XPS contributions for the Fe 2p XPS of Fe_2O_3 including both angular momentum coupling and shake configurations with the CI14 ionic states. The sum of these contribution is included as a solid black line.

Fig. 3. Plot of the integrated Fe 2p XPS intensity, Isum(E), for the energy range for $0 \leq BE(rel) < 40$ eV; (a) SO WFs and (b) CI14 WFs. The total 2p intensity is shown as a black curve and the individual $2p_{3/2}$ and $2p_{1/2}$ contributions are shown as red and blue curves, respectively. The units are percent of total intensity.

Fig. 4. Properties of groups of states in the 4 regions between $0 \leq BE(rel) < 26$ eV for (a) SO WFs and (b) CI14 WFs. The properties are intensity, vertical bars, and $2p_{1/2}$, $2p_{3/2}$, and shake occupations shown as points; the measured 2p XPS is also shown as a black curve. The scale for the occupations is on the left and for the SA intensities, it is on the right.

Fig. 1. Plots of the theoretical predictions for the Fe 2p XPS of Fe_2O_3, with solid curves, compared to experiment, dotted curve: (a) for SO ionic states where only angular momentum is treated and (b) for CI14 ionic states where shake configurations are included. The total predicted XPS is a bold line and large individual contribution for specific final states are in lighter curves, color online. See text for details.

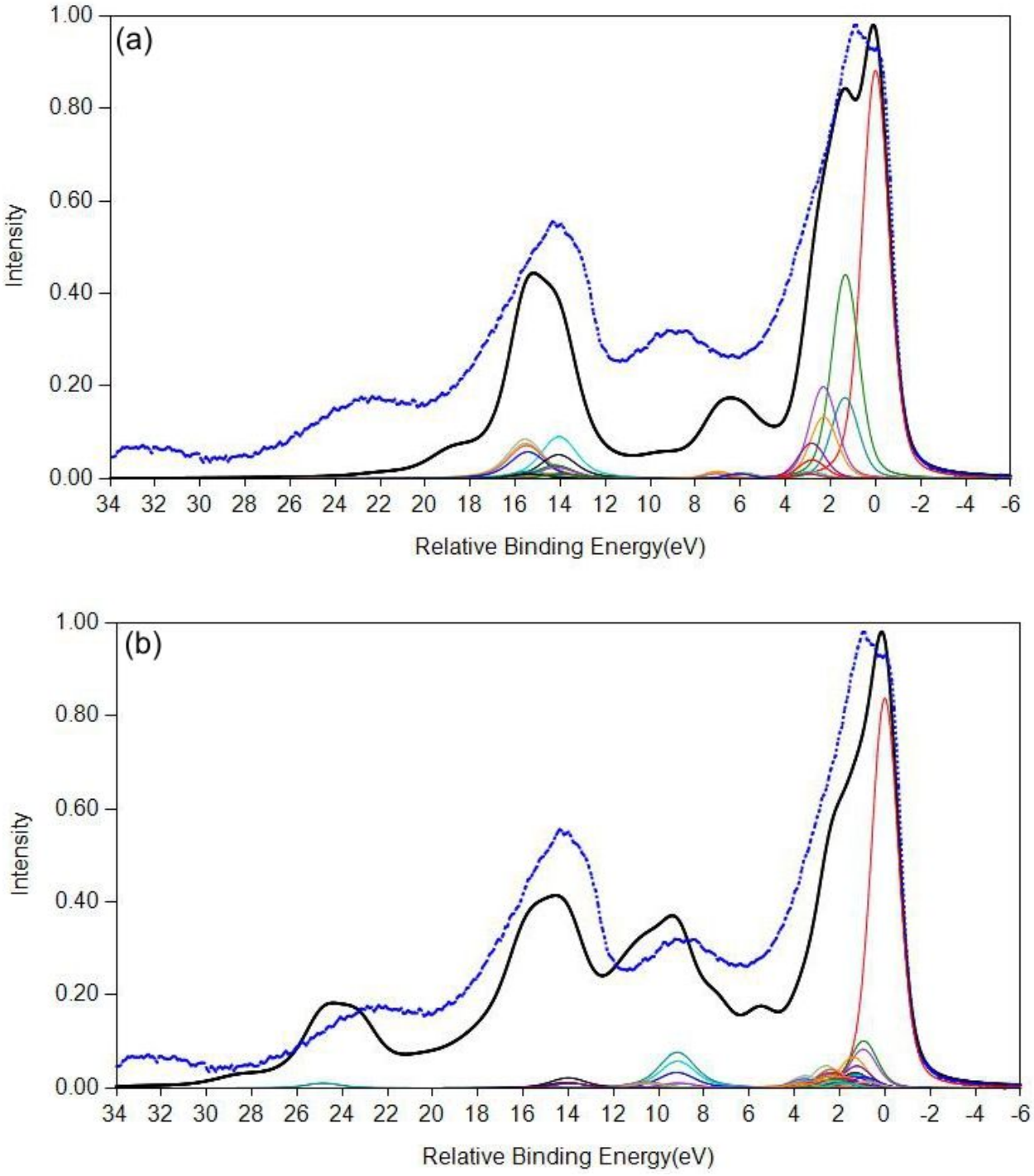

Fig. 2. Plot of the theoretical predictions for the $2p_{1/2}$, dashed blue line, and the $2p_{3/2}$, dashed red line, XPS contributions for the Fe 2p XPS of Fe_2O_3 including both angular momentum coupling and shake configurations with the CI14 ionic states. The sum of these contribution is included as a solid black line.

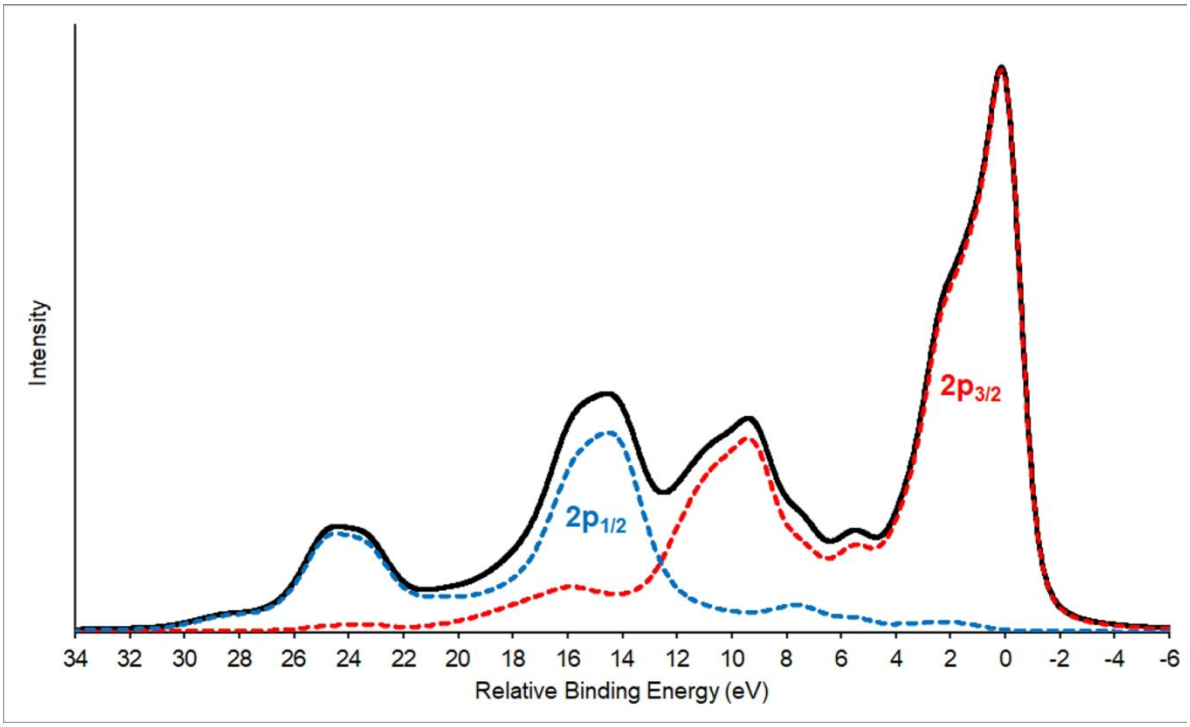

Fig. 3. Plot of the integrated Fe 2p XPS intensity, Isum(E), for the energy range for 0≤BE(rel)<40 eV; (a) SO WFs and (b) CI14 WFs. The total 2p intensity is shown as a black curve and the individual $2p_{3/2}$ and $2p_{1/2}$ contributions are shown as red and blue curves, respectively. The units are percent of total intensity.

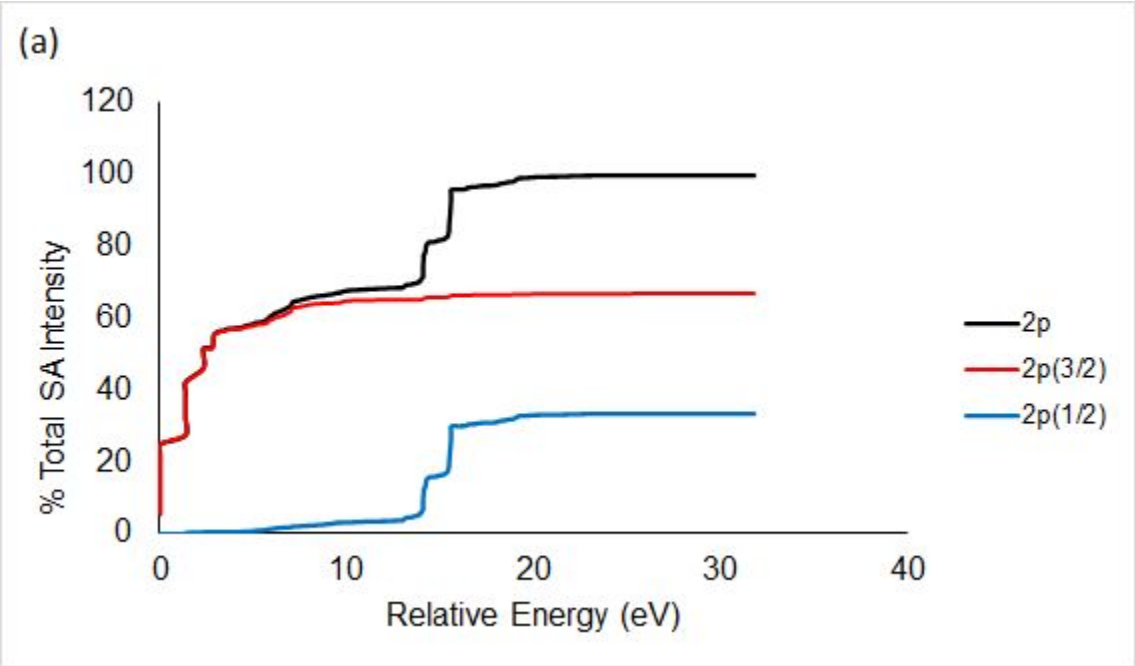

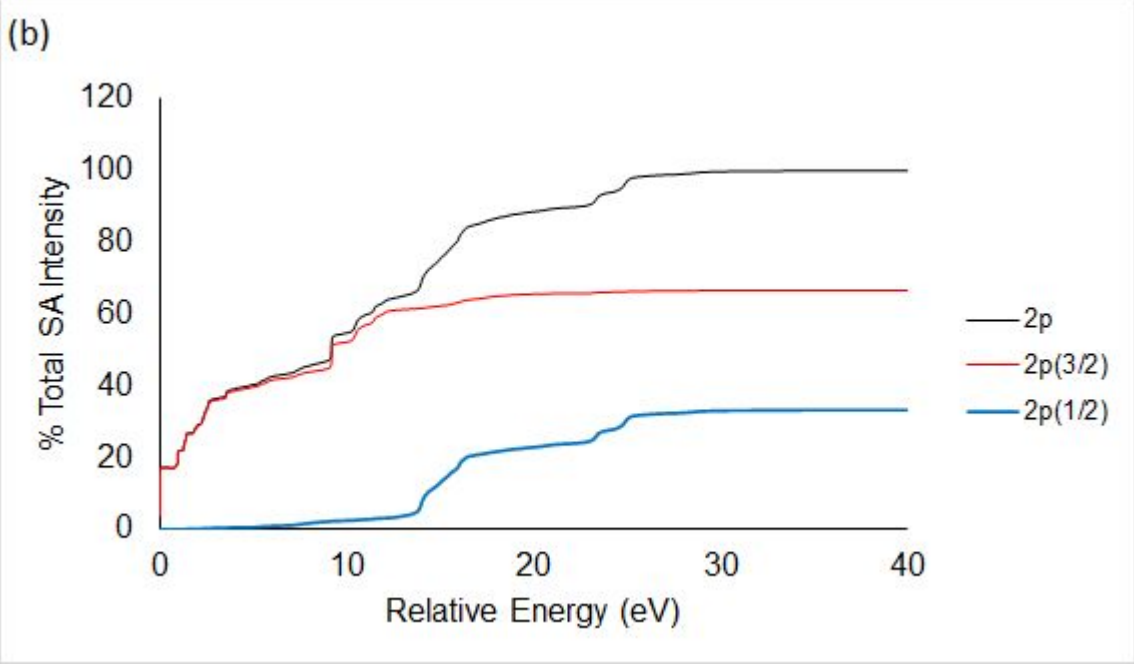

Fig. 4. Properties of groups of states in the 4 regions between 0≤BE(rel)<26 eV for (a) SO WFs and (b) CI14 WFs. The properties are intensity, vertical bars, and $2p_{1/2}$, $2p_{3/2}$, and shake occupations shown as points; the measured 2p XPS is also shown as a black curve. The scale for the occupations is on the left and for the SA intensities, it is on the right.